Trehalose ameliorates severe acute pancreatitis by modulating the gut microbial metabolism

Weiqin Li

liweiqindr@nju.edu.cn

Nanjing University

Haibin Hao

Jinling Hospital https://orcid.org/0000-0002-3206-1874

Deren Du

Jinling Hospital

Hong Lin

Southeast University

Lu Ke

Nanjing University

Aikun Fu

Zhejiang University

Chongli Shi

Shanghai University

Wei Li

Jinling Hospital

Yuanzhen Li

Nanjing University

Gaohuan Hou

Nanjing University

Lianglan Li

Nanjing University

Yuxiu Liu

Jinling Hospital

Shengwen Shao

Huzhou University

Zhihui Tong

Nanjing University

Article

Keywords: Trehalose, Gut microbiota, Severe acute pancreatitis, Gut microbial metabolism

Posted Date: October 1st, 2024

DOI: https://doi.org/10.21203/rs.3.rs-4768563/v1

Additional Declarations: (Not answered)

Abstract

Severe Acute Pancreatitis (SAP) is an acute, severe, and high-mortality special type of pancreatitis, often accompanied by gut microbiota disorders. Gut microbiota and its derived metabolites are involved in SAP progression, but gut microbial metabolism in SAP and their roles remain unclear. In this study, we found that gut microbial metabolism homeostasis was imbalanced in SAP, especially the increase of lipids metabolism and decrease of carbohydrate & amino acid metabolism, which were reversed by depleting the gut microbiota. Trehalose in microbial carbohydrate metabolism significantly increased after depleting gut microbiota. Interestingly, oral trehalose effectively reduced pancreatic injury and ameliorated the SAP-induced microbial metabolism imbalance by increasing carbohydrate metabolism and decreasing lipids metabolism, especially increasing galactose metabolism. The role of trehalose was shown to be dependent on gut microbiota via FMT, especially the inhibition of *Lactobacillaceae* and the expansion of *Muribaculaceae*. Mechanistically, trehalose-remodeled gut microbiota reduced SAP-induced increases in serum TG, IL-6, IL-17A, and TNF-α, and inhibited caspase-3-mediated apoptosis and macrophage infiltration in the pancreas. Overall, our study revealed that trehalose ameliorates SAP by modulating the gut microbial metabolism homeostasis, which provides new insights into alterations of gut microbial metabolism and the “microbial metabolism-gut-pancreatic axis” to treat pancreatic diseases.

Introduction

Acute pancreatitis (AP) is a disease characterized by excessive activation of pancreatic enzymes and a local pancreatic inflammatory response[1]. Approximately 20–30% of patients’ conditions progress to severe acute pancreatitis (SAP), often accompanied by multiorgan failure and infectious complications[2]. Clinical first-line therapeutic measures are still prescribed based on symptoms, and there are no specific drugs available thus far[3]. The prognosis and severity of AP are associated with the gut microbiota[4,5]. The changes in the gut microbiota vary according to the severity of pancreatitis, and the microorganisms showing significant changes in mild, moderate, and severe AP are *Bacteroides, Escherichia-Shigella, and Enterococcus*, respectively[6]. Germ-free mice are less inflamed than SPF mice with AP, and the depletion of gut microbes by broad-spectrum antibiotics in AP mice attenuates pancreatic injury[4]. Therefore, the “microbiota-gut-pancreatic axis” is a potential drug target for treating pancreatitis.

Dietary supplementation is closely related to diseases and has attracted increasing attention. Dietary supplements for enteral nutrition can reduce the incidence of systemic inflammatory response syndrome (SIRS) and organ failure in SAP patients[7,8]. The dietary addition of butyrate effectively reverses intestinal barrier damage and reduces the levels of proinflammatory cytokines induced by SAP[9]. Moreover, our pre-study clinically confirms the role of immune enhancement and enteral nutrition therapy for SAP[10,11]. Dietary supplementation is considered to ameliorate SAP through the “microbiota-gut-pancreatic axis”, mainly by promoting probiotics and inhibiting harmful bacteria. Moreover, a recent study suggested that gut microbial carbohydrate metabolism regulated insulin resistance in the

“microbiota-gut-pancreatic axis”[12]. Dietary supplementation certainly affects gut microbial metabolism when modulating gut microbiota. Therefore, studying the “microbial metabolism-gut-pancreatic axis” of dietary supplementation will improve the application of SAP therapeutics.

Trehalose, a natural carbohydrate, is used as a dietary supplement. It has been reported to be a "sugar of life" and was approved as a safe food additive by the FDA[13]. Previous studies have shown that trehalose has the potential to treat various diseases, such as its anti-tumor, immunomodulatory, and anti-inflammatory effects[14,15]. Trehalose has also been recommended for treating lifestyle-related diseases, such as type 2 diabetes[16,17]. Furthermore, a recent study suggested that natural disaccharides, including trehalose and fibrulose, reshaped the gut microbiota in vitro[18]. Interestingly, we found that in SAP mice, the changes in gut microbial carbohydrate metabolism reversed from a decrease to a significant increase after depletion of gut microbiota, especially trehalose. Combined with the role of trehalose in reshaping gut microbiota[19], we hypothesize that trehalose is involved in the “microbial metabolism-gut-pancreatic axis” in SAP.

Herein, we established a mouse model of SAP using caerulein and lipopolysaccharide (LPS). Using an antibiotic cocktail (ATBx) to treat wild-type (WT) mice, oral trehalose in WT mice and fecal microbiota transplantation (FMT) in germ-free (GF) mice demonstrated that trehalose ameliorated SAP through the “microbiota-gut-pancreatic axis”. Furthermore, we conducted an assessment of alterations in gut microbiota and microbial metabolism using sequencing of 16S ribosomal RNA (rRNA) genes and metabolome data analysis. In this study, we delved into the mechanisms by which SAP-induced alterations in the gut microbial metabolism impact both local and systemic inflammatory responses. Based on our findings, we contribute novel perspectives to the field of SAP treatment, particularly focusing on the role of trehalose in the “microbial metabolism-gut-pancreatic axis”.

Results

Bacterial depletion ameliorates pancreatic injury and the inflammatory response in SAP

To investigate whether the gut microbiota is involved in the progression of SAP, ATBx treatment was used to deplete the gut microbiota of mice (**Supplementary Fig. 1**). Firstly, the WT mice were divided into four groups: the blank control (BC), ATBx, SAP, and ATBx-SAP groups (Fig. 1a). Compared to SAP group, hematoxylin and eosin (H&E) staining revealed that inflammation and necrosis of the pancreas were significantly decreased in ATBx-SAP group (Fig. 1b, c), and serum amylase levels were decreased in ATBx-SAP group (Fig. 1d). These results suggest that bacterial depletion in gut ameliorates pancreatic injury of SAP.

Then all 23 inflammatory mediators were increased in SAP, but the levels of IL-6, IL-17A, IFN-γ, TNF-α, and IL-4 were significantly reduced after ATBx treatment (Fig. 1e). In addition, we previously showed that

high triglyceride (TG) levels affect pancreatic injury in pancreatitis[20]. As shown in Fig. 1f, serum TG and total cholesterol (TC) were higher in SAP, and ATBx treatment significantly reduced serum TG concentration. Our data suggest that bacterial depletion in the gut can ameliorate inflammatory response and metabolic abnormalities of SAP.

Bacterial depletion reverses SAP-induced gut microbial metabolism imbalance

To explore the role of gut microbial metabolism in SAP, the gut microbiota composition and indices of microbial metabolism were analyzed. Across the BC, ATBx, and SAP groups, PCoA analysis revealed a distinct microbial composition among them (Fig. 2a). Taking the BC group as a reference, the top 10 taxonomic phyla and families separately in terms of abundance were presented with the proportion of changes in each group (Fig. 2b). At the phylum level, these was a decrease in the abundances of *Firmicutes* and *Desulfobacterota* and an increase in the abundances of *Proteobacteria* and *Verrucomicrobia* in SAP compared to BC group (LDA score > 3.5) (Fig. 2c). At the family level, these was a decrease in the abundances of *Lachnospiraceae*, *Erysipelotrichaceae*, and *Desulfovibrionaceae* and an increase in the abundances of *Enterobacteriaceae*, *Akkermansiaceae*, *and Lactobacillaceae* in SAP compared to BC group (Fig. 2c). The abundances of *Proteobacteria* and *Enterobacteriaceae* at the phylum and family levels were significantly increased after ATBx treatment, accounting for over 80% in ATBx group and over 60% in ATBx-SAP group (Fig. 2b, d **and Supplementary Fig. 2**). These data suggest that there is significant gut microbiota disorders in SAP and that the gut microbiota is indeed largely depleted after ATBx treatment.

Next, to investigate the impact of SAP-induced gut microbiota disorders on microbial metabolism, metabolomics analysis was used to evaluate changes in the metabolic components of each group. PCA analysis showed a clear separation of the metabolic components among the BC, ATBX, and SAP groups (Fig. 2e**)**. For metabolites with significant changes in abundance in the SAP vs. BC group (fold change $\geq$ 2 or $\leq$ 0.5 and $p \leq 0.001$), we showed the distribution of the top 10 metabolic classes. In the SAP vs. BC group, increased microbial metabolites were dominated by lipids metabolism, with 29.82% and 17.54% of fatty acyls and glycerophospholipids, respectively. And decreased microbial metabolites were dominated by carbohydrate and amino acid metabolism, with 33.33% and 8.51% of carboxylic acids and derivatives and organooxygen compounds, respectively (Fig. 2f). Compared to BC or SAP group, ATBx treatment exhibited opposite differences in the abundances of significantly altered gut microbial metabolites (Fig. 2g **and Supplementary Fig. 3a, b**). These data suggest that gut microbial metabolism is similarly imbalanced along with gut microbiota disorders in SAP.

Indeed, according to the ecological distribution of overall abundance of microbial metabolism in BC mice, the overall abundance of fatty acyls & glycerophospholipids was essentially equal to that of carboxylic acids and derivatives & organooxygen compounds (Fig. 2h). ATBx treatment decreased the overall abundance of microbial metabolism, specifically an increase in fatty acyls & glycerophospholipids and a decrease in carboxylic acids and derivatives & organooxygen compounds (**Supplementary Fig. 3c-**

e). To more directly analyze the effect of ATBx treatment on SAP-induced microbial metabolism imbalance, the metabolites in the intersection of ATBx-SAP vs. SAP group and SAP vs. BC group were analyzed (Fig. 2i). ChemRICH class enrichment showed that SAP-induced changes in microbial metabolism were the opposite of those observed following ATBx treatment (Fig. 2j). Specifically, in carboxylic acids and derivatives & organooxygen compounds, the metabolites showing significantly increased abundances were mainly oligosaccharides and peptides after depleting the gut microbiota, with the significant changes in trehalose (Fig. 2k). This indicates that bacterial depletion reverses SAP-induced microbial metabolism imbalances (Fig. 2l). Based on these data, we hypothesized that trehalose in oligosaccharides is involved in the progression of SAP.

Trehalose ameliorates the severity of severe acute pancreatitis

Trehalose has been shown to play a beneficial role in the treatment of various diseases[21]. Combined with the previous results, we further determined whether trehalose has a beneficial role in SAP. WT mice were randomized into the BC, trehalose (Tre), SAP, and Tre-SAP groups, and a graded dose of trehalose was orally administered daily for 15 days (Fig. 3a). The possible effects of trehalose was excluded by adding a 0.2% trehalose group. Compared to the SAP group, pancreatic inflammation, and necrosis were significantly alleviated in the Tre-SAP group with 0.2%, 0.5%, 1%, or 2% trehalose (Fig. 3b, c). Oral 5% trehalose did not change the pathology scores of SAP, and we found that 5% trehalose can cause diarrhea and increased urine output in SAP. Serum amylase levels were not altered after trehalose treatment (Fig. 3d). These data confirm that trehalose can ameliorate pancreatic injury in SAP.

Next, according to the inflammatory cytokines profile, 0.2% trehalose significantly reduced the expression of TNF-α, MCP-1, IL-6, and IL-17A in SAP, and MCP-1 and TNF-α levels were significantly reduced in the Tre group compared to BC group (Fig. 3e-g). In addition, trehalose treatment effectively reduced SAP-induced increases in TG levels but not TC levels (Fig. 3h). These findings suggest that trehalose treatment ameliorates inflammatory response and metabolic abnormalities of SAP.

Trehalose modulates the gut microbial metabolism homeostasis in SAP

Considering the significant change in trehalose observed in the ATBx-SAP group, we further explored whether trehalose could act on the gut microbiota and microbial metabolism. Differences in the gut microbiota and microbial metabolism were analyzed among the BC, 0.2% Tre, SAP, and 0.2% Tre-SAP groups. PCoA analysis showed that the gut microbiota among the BC, 0.2% Tre, and SAP groups were entirely separated (Fig. 4a). First, the gut microbiota disorders of SAP in the phyla and families were consistent with previous descriptions (**Supplementary Fig. 4**). At the phylum level, there was an increase in the abundances of *Bacteroidota* and *Proteobacteria* and a decrease in the abundances of *Firmicutes* and *Deferribacterota* in the Tre group compared to BC group, and trehalose significantly promoted the abundance of *Bacteroidota* and suppressed *Firmicutes* in SAP group (Fig. 4b-d, **Supplementary Fig. 4a, b**). At the family level, the abundance of *Muribaculaceae* increased, whereas that of *Lactobacillaceae*

decreased in the Tre or Tre-SAP group (Fig. 4b-d, **Supplementary Fig. 4c, d**). Taken together, these findings confirm that oral trehalose can modulate gut microbiota disorders, specifically the expansion of *Muribaculaceae* and inhibition of *Lactobacillaceae*.

Next, PCA analysis revealed a small difference between SAP and Tre-SAP groups (Fig. 4e). Compared to BC group, the increased metabolites in SAP group were predominantly fatty acyls & glycerophospholipids, and the decreased were predominantly carboxylic acids and derivatives & organooxygen compounds, which is consistent with previous data (Fig. 4f). According to the previous screening criteria (fold change ≥ 2 or ≤ 0.5 and $p \leq 0.001$), there were few significantly different metabolites in Tre-SAP vs. SAP group (Fig. 4g and **Supplementary Fig. 5a**). These suggested that trehalose treatment did not cause dramatic significant changes in gut microbial metabolism as ATBx treatment. Therefore, we choose another commonly used analytical model, OPLS-DA model (**Supplementary Fig. 5b**). Trehalose treatment significantly altered the abundances of 74 metabolites in the intersection of Tre-SAP vs. SAP group and Tre vs. BC group (VIP ≥ 1) (**Supplementary Fig. 5c**). Carboxylic acids and derivatives & organooxygen compounds were the main classes in increased metabolites, while carboxylic acids and derivatives & fatty acyls were the main classes in decreased metabolites (**Supplementary Fig. 5d**). Moreover, the abundances of 93 metabolites were significantly altered in the intersection of Tre-SAP vs. SAP group and SAP vs. BC group (VIP ≥ 1) (Fig. 4h). Trehalose treatment increased the abundances of organooxygen compounds inhibited in SAP group, and decreased the abundances of fatty acyls elevated in SAP group (Fig. 4i). ChemRICH class enrichment also showed that trehalose treatment resulted in decreased abundance of fatty acyls and increased abundance of organooxygen compounds in Tre-SAP group compared to SAP group (Fig. 4j-k). These results indicate that trehalose ameliorates SAP by modulating gut microbial metabolism, specifically increasing carbohydrate metabolism and decreasing lipids metabolism.

Furthermore, for significantly different metabolites after trehalose treatment, pathway enrichment analysis revealed that the pathways significantly associated with trehalose were galactose metabolism, pentose phosphate pathway, and biosynthesis of unsaturated fatty acids ($p < 0.01$) (Fig. 4m). The metabolites related to trehalose were D-(+)-galactose and inositol in galactose metabolism, which were increased by trehalose in the Tre-SAP vs. SAP group compared to SAP vs. BC group (Fig. 4n). In the biosynthesis of unsaturated fatty acids, 16-hydroxyhexadecanoic acid, arachidonic acid and 8Z,11Z,14Z-eicosatrienoic acid were decreased by trehalose (Fig. 4n). Similarly, D-(+)-galactose was increased in the intersection of Tre-SAP vs. SAP group and SAP vs. BC group **(Supplementary Fig. 5e)**. Taken together, these findings suggest that galactose metabolism is a key factor in the trehalose-mediated “microbial metabolism-gut-pancreatic axis”.

Trehalose ameliorates SAP in a gut microbiota-dependent manner

To further verify whether the role of trehalose depends on gut microbiota, we conducted FMT from BC or Tre mice to GF mice and labeled them "BC-FMT" or "Tre-FMT" group, respectively (Fig. 5a). First, in GF

mice, oral trehalose did not ameliorate SAP but instead increased serum keratinocyte-derived chemokine (KC) and IL-10 levels (Fig. 5b-e). After FMT, pancreatic inflammation, and necrosis were significantly increased in the BC-FMT-SAP compared to the SAP group, and their pathological scores in the Tre-FMT-SAP group were lower than those in the BC-FMT-SAP group (Fig. 5b, c). Consistent with oral trehalose, trehalose-remodelled microbiota failed to reduce serum amylase levels in Tre-FMT-SAP group (Fig. 5d). Moreover, serum TNF-α, IL-6 and IL-17A were decreased in the Tre-FMT-SAP group compared to BC-FMT-SAP group (Fig. 5f). The serum TG level increased after FMT in GF mice, and the trehalose-remodelled microbiota modulated this change (Fig. 5g). These data confirm that the role of trehalose in SAP depends on gut microbiota.

Galactose metabolism and Muribaculaceae are key factors in trehalose-induced "microbial metabolism-gut-pancreatic axis"

To further understand the effect of trehalose on the "microbial metabolism-gut-pancreatic axis" in SAP, gut microbiota and microbial metabolism were analyzed after FMT in GF mice. There were some differences in the gut microbiota between BC-FMT-SAP and Tre-FMT-SAP groups (Fig. 6a). From the top 10 phyla (families) in terms of abundance, as in WT mice, *bacteroidota (Muribaculaceae)*, *Verrucomicrobiota (Akkermansiaceae)* and *Firmicutes (Lactobacillaceae)* were still overwhelmingly dominant in gut microbiota after FMT in GF mice (Fig. 6b). Based on LEfSe analysis at the phylum and family levels (LDA score > 3.5), these were increased abundances of *Bacteroidota* and *Muribaculaceae* and a decreased abundances of *Firmicutes* and *Lactobacillaceae* in Tre-FMT-SAP group compared to BC-FMT-SAP group (Fig. 6c). These findings are consistent with the results of oral trehalose, further confirming that *Muribaculaceae* was the key factor in the role of trehalose.

Next, there was also a significant difference in gut microbial metabolism between BC-FMT-SAP and Tre-FMT-SAP groups (Fig. 6d, e). From ChemRICH class enrichment analysis of 134 differential metabolites (VIP ≥ 1), the abundances of organooxygen compounds & carboxylic acids and derivatives & glycerophospholipids were increased while the fatty acyls decreased in Tre-FMT-SAP group compared to BC-FMT-SAP group (Fig. 6f). For the 19 significantly different metabolites in Tre-FMT-SAP vs. BC-FMT-SAP group (VIP ≥ 1 and $p < 0.05$), the most significant pathway enrichment was that of galactose metabolism (Fig. 6g, h). These data confirm that galactose metabolism in the gut was a key factor in the role of trehalose.

To clarify whether there is a correlation between *Muribaculaceae* and *Lactobacillaceae* and significantly different metabolites, a network heatmap was performed. *Muribaculaceae* was positively correlated with these metabolites, while *Lactobacillaceae* was negatively correlated, and D-(+)-galactose (galactose metabolism) and 16-hydroxy hexadecanoic acid (biosynthesis of unsaturated fatty acids) were negatively correlated, which was consistent with the results for oral trehalose (Fig. 6i). Thus, we propose that galactose metabolism and *Muribaculaceae* in gut microbiota are key factors in trehalose-mediated "microbial metabolism-gut-pancreatic axis".

Trehalose reduces macrophage infiltration and caspase-3-mediated apoptosis in the pancreas

The innate immune response, dominated by macrophages and neutrophils, is closely related to the severity of acute pancreatitis[22]. F4/80 and MPO expressions were detected in the pancreas. After ATBx treatment, immunohistochemistry (IHC) and immunofluorescence (IF) showed that pancreatic F4/80 and MPO expressions were decreased in ATBx-SAP group compared to SAP group (Fig. 7a). SAP-induced high expression of F4/80 was inhibited by oral trehalose or trehalose-remodeled gut microbiota, whereas MPO expression was not affected by oral trehalose or trehalose-remodeled gut microbiota (Fig. 7b-d). These data suggest that macrophage infiltration in the pancreas was decreased by trehalose, while neutrophil infiltration was not. Therefore, trehalose ameliorates SAP-induced inflammation by regulating macrophage.

The two programmed cell death pathways, autophagy and apoptosis, are considered to be associated with the progression of pancreatitis[23]. To determine whether the role of trehalose was related to cell apoptosis and autophagy, we examined the expression levels of Bcl-2, caspase-3, and Beclin1. Bcl-2, caspase-3, and Beclin1 expression were increased in the SAP group compared to the BC group (Fig. 8a-c). Notably, SAP-induced high expression of caspase-3 was significantly decreased by ATBx treatment, oral trehalose, and trehalose-remodelled gut microbiota, while Bcl-2 and Beclin1 expression were not affected (Fig. 8a-c). Based on the quantitative analysis of IHC and IF, SAP-induced high expression of caspase-3 was inhibited in the ATBx-SAP, Tre-SAP, and Tre-FMT-SAP group (Fig. 8d, e). Although the changes in Bcl-2 expression were not statistically significant ($p > 0.05$), there was a tendency toward increased Bcl-2 expression levels in the ATBx-SAP, Tre-SAP, and Tre-FMT-SAP group (Fig. 8d, e). Consistent with IHC and IF results, western blotting showed that SAP-induced high-cleaved caspase-3 expression was decreased by ATBx treatment, oral trehalose, and trehalose-remodelled gut microbiota while pro-caspase-3 expression was increased (Fig. 8f). These results suggest that trehalose ameliorates SAP-induced necrotic by regulated the caspase-3-mediated apoptosis.

Additionally, we found that Beclin1, caspase-3, and MPO were also expressed in pancreatic islets, with Beclin1 in α cells, caspase-3 in α/β cells, and MPO in β cells (**Supplementary Fig. 6**). Beclin1 and MPO levels in islets did not change during SAP progression, but caspase-3 expression in islets was increased in SAP group compared to BC group, which was inhibited by ATBx treatment. Oral trehalose or trehalose-remodeled gut microbiota did not affect SAP-induced caspase-3 expression increase in islet. These findings imply that gut microbiota are involved in islet injury during SAP progression.

Discussion

Herein, we discovered a new function of trehalose, demonstrating its potential to ameliorate SAP through its interaction with the gut microbiota and microbial metabolism (**Fig. 9**). We found that ATBx treatment, oral trehalose treatment, and trehalose-remodeled gut microbiota directly increased the abundances of

carbohydrate metabolism and reduced lipids metabolism to improve the gut microbial metabolism imbalance and inhibit inflammatory cytokines and cell apoptosis to ultimately ameliorate SAP. Overall, the findings indicating the potential beneficial impact of trehalose treatment on SAP suggest that trehalose could serve as a novel gut microbiota-dependent dietary supplement for SAP treatment.

Trehalose, an FDA-approved drug, is utilized for the treatment of nervous system diseases and is widely acknowledged as a multitarget therapeutic agent[24,25]. Significantly, trehalose has been shown to have positive effects on a mouse model of caerulein-induced AP[26]. However, the specific molecular mechanisms underlying the effects of trehalose treatment remain undetermined. In this study, we confirmed the ameliorating effects of trehalose treatment on pancreatitis and explored the underlying molecular mechanisms involved. Disturbances in the gut microbiota during the pathogenesis and development of SAP have received extensive research attention[4,6]. Furthermore, potential therapeutic targets of the microbiota-gut-pancreatic axis, which modulates the gut microbiota and its metabolites, are considered to hold promise as medical treatments for SAP[27]. We first observed that the gut microbial metabolism imbalance in SAP mice was reversed after gut microbiota depletion, with significant changes in the abundances of oligosaccharides, including trehalose. Indeed, trehalose treatment can modulate microbial metabolism imbalances and increase the abundance of the gut probiotic *Muribaculaceae*. By transplanting the trehalose-remodeled gut microbiota to GF recipients, we confirmed the direct role of the trehalose-remodeled gut microbiota in modulating inflammatory reactions and hyperlipidemia in SAP. Notably, we observed a consistent enrichment of *Muribaculaceae*, accompanied by increased abundances of organooxygen compounds and decreased abundances of fatty acyls in WT and GF SAP mice models. These findings suggest that dietary trehalose treatment can reverse SAP-induced gut microbial metabolism imbalance and gut microbiota disorders, thereby ameliorating SAP.

Recent research has demonstrated that trehalose treatment can reshape the gut microbiota[18], but the role of trehalose treatment in SAP-induced gut microbiota disorders remains unclear. The gut microbiota showed an increase in the abundance of *Proteobacteria* and a decrease in the abundance of *Firmicutes* in SAP mice and humans[28,29], which is consistent with our results. We found that trehalose treatment increased the abundance of *Bacteroidota* and decreased the abundance of *Firmicutes* in SAP, and *Muribaculaceae* was the main dominant bacterium in *Bacteroidota*. We consider that *Muribaculaceae* may be a key trehalose-related bacterium involved in the microbiota-gut-pancreatic axis. *Muribaculaceae* has previously been revealed to be involved in the degradation of carbohydrates in the gut and the beneficial effects of dietary polysaccharides[30,31]. Our data further confirmed through trehalose-remodeled FMT in GF mice that trehalose treatment ameliorates SAP by increasing *Muribaculaceae* abundance.

Gut microbiota-derived metabolites, such as bile acids, peptidoglycans, and SCFAs, act as key regulators of metabolic disorders[32]. Recent studies have suggested that gut microbiota-derived metabolites were associated with the severity of acute pancreatitis[5,33], but gut microbial metabolism abnormalities in SAP have not been described in detail. In this study, we first observed a severe imbalance in gut microbial

metabolism accompanied by gut microbiota disorders in SAP mice, specifically an increase in lipids metabolism and a decrease in carbohydrate & amino acid metabolism. Moreover, trehalose treatment was found to ameliorate inflammation and lipids metabolism in mice and humans with hyperlipidemia or hyperglycemia[34–36]. Similar to these observations, we not only found that oral trehalose treatment ameliorated inflammation, necrosis, and hyperlipidemia in SAP but also partially restored the SAP-induced microbial metabolism imbalance. Specifically, trehalose reduced serum MCP-1, IL-1β, IL-6, and TNF-α levels to regulate the inflammatory response[15,37]. Our data further confirmed that in the "microbial-gut-pancreas axis", trehalose exerted anti-inflammatory effects by decreasing IL-17A, IL-6, and TNF-α levels. A recent study demonstrates that gut microbial carbohydrate metabolism plays a role in the development of insulin resistance[12]. Similarly, we observed that microbial carbohydrate metabolism increased and lipid metabolism decreased after oral trehalose treatment in SAP progression. *Muribaculaceae* in gut microbiota was positively correlated with the abundance of D-(+)-galactose and negatively correlated with that of 16-hydroxyhexadecanoic acid. Thus, our findings demonstrate a relationship between dietary supplementation, gut microbial metabolism, and gut microbiota, highlighting the essential interconnection between gut microbial metabolism and the development of SAP, i.e., the "microbial metabolism-gut-pancreatic axis".

In this study, we revealed that the trehalose-mediated microbial-gut-pancreas axis decreased macrophage infiltration and apoptosis, which is considered the main mechanism by which trehalose treatment ameliorates pancreatic inflammation and necrosis in SAP. A recent study reported that glucocorticoids inhibited LPS-induced macrophage-associated inflammatory immune responses through metabolic rewiring[38]. Similarly, we revealed that trehalose inhibited macrophage infiltration via gut microbial metabolism homeostasis in caerulein & LPS-induced SAP mice. Studies involving multiple organs have also demonstrated that trehalose treatment inhibits cell apoptosis[39–41]. Consistent with these results, we showed that trehalose increased Bcl-2 and decreased caspase-3 activation but had no effect on Beclin-1 expression, suggesting that trehalose treatment ameliorates pancreatic injury by inhibiting caspase-3-mediated apoptosis in SAP. Although trehalose treatment has been reported to modulate pancreatic islet function in diabetes[36], we only found a correlation between gut microbiota and pancreatic islet injury and did not observe a role for oral trehalose on islet injury in SAP. However, our study provides new insights into the mechanism of trehalose-mediated amelioration in SAP.

Several worldwide clinical trials have explored the potential of trehalose for treating a range of conditions, such as Alzheimer's disease, cardiovascular diseases, dry eye disease, and infertility (https://www.clinicaltrials.gov/), and the injectable trehalose drug SLS-005 has been approved by the FDA for the treatment of spinocerebellar ataxia type 3[42]. Although much preclinical evidence has suggested the beneficial effects of trehalose, trehalose has been reported to be associated with the prevalence of *Clostridioides difficile* infection, but it is still controversial[19,43]. Surprisingly, we observed that oral 5% trehalose did not ameliorate SAP but instead caused diarrhea and increased urine output in mice, which may be related to gut disruption induced by a high-sugar diet[44]. Thus, our findings also support the role of trehalose for clinical application in SAP.

In general, we provide new insights into the physiological roles of trehalose from three perspectives: gut-blood-pancreas, and trehalose treatment modulates the gut microbial metabolism imbalance to ameliorate SAP. These discoveries not only have potential implications for the use of trehalose as a therapy for SAP but also offer new insights into the “microbial metabolism-gut-pancreatic axis”.

Methods

Animal experiments

Six-week-old female C57BL/6J mice were obtained from GemPharmatech Co., Ltd. (Nanjing, China) and housed under specific pathogen-free (SPF) conditions. All mice were acclimatized to the laboratory environment for at least 3 days before they entered the experiment. The animal experiment protocol was approved by the Animal Ethics Committee of Jinling Hospital (Approved No. 2022DZGKJDWLS-0055). At least 2–3 biological replicates were performed for each experiment.

For the antibiotic cocktails treatment (ATBx) group[45], a combination of vancomycin (50 mg/mL, Meilunbio, China, Cat. MB1260), imipenem/cilastatin (25 mg/mL, Merck & Co., USA, ATC No. J01DH51), neomycin (10 mg/mL, Sangon Biotech, China, Cat. A610366), and amphotericin (1 mg/mL, Sangon Biotech, China, Cat. A610030) was given daily by gavage for 5 consecutive days. Moreover, a combination of vancomycin (0.5 mg/mL), imipenem/cilastatin (0.5 mg/mL), neomycin (1 mg/mL), and amphotericin (0.5 μg/mL) was also added to the drinking water.

For the trehalose (Tre) (MCE, USA, Cat. HY-N1132) diet group, the mice continued to drink water containing 0.2%, 0.5%, 1%, 2%, or 5% trehalose for 15 days.

Severe acute pancreatitis model

Caerulein (NJPeptide, Chian, Cat. Pep03263) was injected intraperitoneally according to body weight (300 μg/kg). There was one injection given per hour for seven total injections. A single intraperitoneal injection of LPS (10 mg/kg, MCE, USA, Cat. HY-D1056) was administered one hour after the last caerulein injection. The control group was injected with an equal amount of phosphate-buffered saline (PBS). The first injection of caerulein was administered at 0 h, and the mice were sacrificed after 24 h to obtain the pancreas, serum, cecum, and intestinal fecal contents.

Histopathological evaluation

Pancreatic tissues were fixed in 4% paraformaldehyde for 24 h. The specimens were embedded in paraffin and sectioned (thickness 4 μm). Sections were stained with hematoxylin and eosin (HE) for pathological histological examination. Ten microscopic fields of view (200× magnification) were randomly selected from each section. Each section was scored by three independent investigators using a previously established scoring system for histopathology as follows: edema (0–4 scale), number of acinar necrotic cells (0–4 scale), number of intralobular or perivascular leukocytes (0–4 scale), and hemorrhage and fat necrosis (0–4 scale)[46].

Fecal microbial transplantation (FMT)

Five-week-old female germ-free mice were obtained from GemPharmatech Co., Ltd. (Nanjing, China). First, six-week-old female C57BL/6J mice were fed 0.2% trehalose in drinking water for 15 days. Then, their intestinal fecal contents were placed in a fecal microbial protection solution (saline containing 30% glycerol and 0.1% cysteine). The fecal microbial protection solution was added at a ratio of 1:3. Then, each germ-free mouse was administered 20 μL/g fecal suspension 3 times a week by gavage. The fecal microorganisms for each gavage were a mix of the intestinal fecal contents of five C57BL/6J mice.

16S rRNA gene sequencing analysis

Total microbial DNA was extracted from fecal contents using a Magnetic Soil and Stool DNA Kit (TianGen, China). DNA purity and concentration were then checked by electrophoresis on a 1.2% agarose gel. DNA samples were used as templates for PCR amplification of the V4 region of the bacterial 16S rRNA gene. According to the requirements of the Illumina NovaSeq sequencing platform, two-way sequencing was performed, and libraries were constructed using a two-step PCR amplification method with a TruSeq® DNA PCR-Free Sample Preparation Kit (San Diego, USA). The PCR amplification products were recovered with an AXYGEN AxyPrepDNA Gel Recovery Kit (California, USA) and quantified with an FTC-3000™ real-time PCR instrument.

The sequencing of PCR amplification products was performed on an Illumina NovaSeq 6000 platform at Novozymes Technology Co. (Beijing, China). The raw data obtained from sequencing were spliced and filtered to obtain clean data. Operational taxonomic unit (OTU) clustering was performed with 97% identity. Species annotation was performed on the OTU sequences, and species annotation analysis was performed using the SSUrRNA database of SILVA138 (http://www.arb-silva.de/) using the Mothur method (threshold value of 0.8-1). Rapid multiple sequence alignment was performed using MUSCLE (version 3.8.31, http://www.drive5.com/muscle/) software to obtain the phylogenetic relationships of all representative OTU sequences. Beta diversity index intergroup variance analysis using R software and LEfSe analysis using linear discriminant analysis (LDA) effect size (LEfSe) software were performed (LDA score (log10) = 3.5 as the cut-off value).

Metabolomic analysis

Metabolomics based on ultrahigh-performance liquid chromatography (UHPLC) coupled with high-resolution mass spectrometry (MS) was performed by Novozymes Technology Co. (Beijing, China). 100 mg samples containing fecal contents were individually ground with liquid nitrogen, and the homogenate was resuspended in prechilled 80% methanol by vortexing. Some of the supernatants were diluted to a final concentration of 53% methanol with LC-MS grade water. Finally, the supernatant was injected into the LC-MS/MS system for analysis.

The raw UHPLC-MS/MS data were imported into Compound Discoverer 3.1 software, and the spectra were processed and compared with the mzCloud, mzVault, and Masslist databases. The raw quantitative results were normalized to obtain the identification and relative quantitative data of the metabolites.

MetaX was utilized to preprocess the data and conduct principal component analysis (PCA) as well as orthogonal partial least squares discriminant analysis (OPLS-DA) to derive the variable importance in projection (VIP) scores for each metabolite. The *p*-value was calculated for each metabolite between the two groups based on univariate analysis (t-test). The default criteria for differential metabolites screening were VIP ≥ 1 & *p*-value < 0.05 or fold change (FC) ≥ 2 or FC ≤ 0.5 & *p*-value < 0.001. Chemical similarity enrichment analysis was performed using ChemRICH (http://chemrich.fiehnlab.ucdavis.edu/)[47]. Pathway enrichment analysis was conducted using MetaboAnalyst 6.0[48].

Inflammatory cytokine analysis

A Bio-Plex Pro Mouse Cytokine 23-plex Assay Kit (California, USA) was used to measure the levels of 23 inflammatory cytokines profile, including IL-1α, IL-1β, IL-2, IL-3, IL-4, IL-5, IL-6, IL-9, IL-10, IL-12 (p40), IL-12 (p70), IL-13, IL-17A, eotaxin, G-CSF, GM-CSF, IFN-γ, KC, MCP-1 (MCAF), MIP-1α, MIP-1β, RANTES and TNF-α. Assays based on liquid chip technology was performed on a Luminex 200 System by Shanghai Universal Biotech Co. (Shanghai, China).

Lipid analysis

The biochemical assessment of lipids followed the World Health Organization lipid reference standards. Low-density lipoprotein cholesterol (LDL-C), high-density lipoprotein cholesterol (HDL-C), triglyceride (TG), and total cholesterol (TC) concentrations were measured enzymatically using a Hitachi 7600 automated analyzer (Kyowa, Japan). Mouse serum was assayed within 30 min of sample collection.

Immunohistochemical analysis

After paraffin block dewaxing and rehydration, the pancreatic tissue was blocked with 5% bovine serum albumin for 30 min and washed with PBS. The tissue sections were incubated with antibodies against Bcl-2 (1:1000, Servicebio, Cat. GB114830), Beclin-1 (1:1000, Servicebio, Cat. GB11228), caspase-3 (1:100, Servicebio, Cat. GB11009-1), MPO (1:500, Servicebio, Cat. GB11224) and F4/80 (1:500, Servicebio, Cat. GB113373) for 12 h. After the membranes were washed 3 times with PBS, they were incubated with a peroxidase-conjugated secondary antibody for 2 h. Staining was monitored under a microscope and terminated when adequate. The slides were then dehydrated and stored. Tissue images were obtained using a microscope (400× magnification). The intensity of specific staining was measured using Image-Pro Plus 6.0 (Media Cybernetics, Silver Spring, MD, USA). Ten fields of view were randomly selected for each section. For Bcl-2, caspase-3, and Beclin-1, the ratio of the area of the positively stained object to the total view area was measured. For MPO and F4/80, the number of positively stained cells was measured. All images were acquired using the same microscope and camera.

Immunofluorescence staining

The tissue was embedded in paraffin and then sectioned to a thickness of 4 μm. Antigen retrieval was performed using EDTA antigen retrieval solution, followed by blocking nonspecific binding with 3% BSA for 30 min. Subsequently, the tissues were incubated with antibodies against Bcl-2 (1:800, Servicebio,

Cat. GB114830), Beclin-1 (1:1000, Servicebio, Cat. GB11228), caspase-3 (1:200, Servicebio, Cat. GB11009-1), MPO (1:500, Servicebio, Cat. GB11224) and F4/80 (1:500, Servicebio, Cat. GB113373) overnight at 4°C. After a 1-h incubation with CY3-conjugated secondary antibodies (Servicebio), the tissues were counterstained with DAPI to visualize the nuclei. Subsequently, images were acquired using a fluorescence microscope (Nikon Eclipse C1, Nikon, Japan). Image-Pro Plus 6.0 was used to analyze the fluorescence intensity.

Western blot analysis

Total protein was obtained from pancreatic tissue with a low-temperature tissue grinder. According to our previously described methods[49], an equal quantity of protein from each sample was subjected to 10% SDS—PAGE and subsequent Western blot assays using anti-Bcl-2 (1:1000, Abways, Cat. CY6717), anti-Beclin-1 (1:1000, ABclonal, Cat. A11761), anti-caspase-3 (1:1000, Proteintech, Cat. 66470–2-Ig) and anti-Tubulin (1:10000, Proteintech, Cat. 66031-1-IG) antibodies. Following incubation with the corresponding secondary antibody, the bands were detected using enhanced chemiluminescence (ECL) reagents. Three bio-repeats were performed in WB analysis.

Statistical analysis

The data are presented as the means ± SEMs. Differences between the two groups were assessed using a two-tailed unpaired Student's t-test. Differences in more than two groups were assessed using analysis of variance (ANOVA), and multiple comparisons were performed for all pairs using the Tukey—Kramer test. For the analysis of the microbiota sequencing data, a two-tailed Wilcoxon rank-sum test was performed between the two groups. $p < 0.05$ was considered to indicate a significant difference. Statistical analysis and graphing were performed using R software (v 4.2.2) and GraphPad Prism (v 8.0.2).

Declarations

Authors' contributions

W.Q.L. and Z.H.T. : conceptualization, funding acquisition, and methodology. S.W.S.: conceptualization, visualization, and methodology. H.B.H. and D.R.D.: Conceptualization, project administration, writing – original draft, writing – review & editing. H.L. : Data curation, Methodology, Writing – review & editing. W.L. and Y.Z.L. : Data curation, methodology. G.H.H. : Data curation, Writing – review & editing. Y.X.L. and C.L.S.: Software, Data curation, Investigation. L.L.L. : Resources, Supervision. L.K. :Conceptualization, supervision, writing–review & editing. A.K.F. : Conceptualization, Writing – review & editing.

Availability of data and materials

All 16S rRNA gene sequences data were obtained from the National Genomics Data Center (NGDC), part of the China National Center for Bioinformation (CNCB) database under accession code

PRJCA026291 (https://ngdc.cncb.ac.cn/gsa/s/xBuNeR5u).

Acknowledgments

We thank Prof. Yangchao Chen from The Chinese University of Hong Kong for suggestions on data presentation. This work was supported by grants from the National Natural Science Foundation of China (82270678, 82102275, and 82070669)

Ethics approval and consent to participate

The animal experiment protocol was approved by the Animal Ethics Committee of Jinling Hospital (Approved No. 2022DZGKJDWLS-0055).

Competing interests

The authors declare no competing interests.

References

1. Boxhoorn, L. et al. Acute pancreatitis. *Lancet*. **396**, 726-734 (2020).
2. Schepers, N. J. et al. Impact of characteristics of organ failure and infected necrosis on mortality in necrotising pancreatitis. *Gut*. **68**, 1044-1051 (2019).
3. Gliem, N., Ammer-Herrmenau, C., Ellenrieder, V. & Neesse, A. Management of Severe Acute Pancreatitis: An Update. *Digestion*. **102**, 503-507 (2021).
4. Zhu, Y. et al. Gut microbiota dysbiosis worsens the severity of acute pancreatitis in patients and mice. *J. Gastroenterol.* **54**, 347-358 (2019).
5. Ammer-Herrmenau, C. et al. Gut microbiota predicts severity and reveals novel metabolic signatures in acute pancreatitis. *Gut*. **73**, 485-495 (2024).
6. Yu, S. et al. Identification of Dysfunctional Gut Microbiota Through Rectal Swab in Patients with Different Severity of Acute Pancreatitis. *Dig. Dis. Sci.* **65**, 3223-3237 (2020).
7. Li, H. et al. Bifidobacterium spp. and their metabolite lactate protect against acute pancreatitis via inhibition of pancreatic and systemic inflammatory responses. *Gut Microbes*. **14**, 2127456 (2022).
8. Mei, Q. X. et al. Pretreatment with chitosan oligosaccharides attenuate experimental severe acute pancreatitis via inhibiting oxidative stress and modulating intestinal homeostasis. *Acta Pharmacol. Sin.* **42**, 942-953 (2021).
9. Zhao, H. B., Jia, L., Yan, Q. Q., Deng, Q. & Wei, B. Effect of Clostridium butyricum and Butyrate on Intestinal Barrier Functions: Study of a Rat Model of Severe Acute Pancreatitis With Intra-Abdominal Hypertension. *Front. Physiol.* **11**, 561061 (2020).
10. Ke, L. et al. Immune enhancement in patients with predicted severe acute necrotising pancreatitis: a multicentre double-blind randomised controlled trial. *Intensive Care Med.* **48**, 899-909 (2022).

11. Sun, J. K. et al. Early enteral nutrition prevents intra-abdominal hypertension and reduces the severity of severe acute pancreatitis compared with delayed enteral nutrition: a prospective pilot study. *World J. Surg.* **37**, 2053-2060 (2013).
12. Takeuchi, T. et al. Gut microbial carbohydrate metabolism contributes to insulin resistance. *Nature*. **621**, 389-395 (2023).
13. Ohtake, S. & Wang, Y. J. Trehalose: current use and future applications. *J. Pharm. Sci.* **100**, 2020-2053 (2011).
14. Del, B. B., Gamberucci, A., Marcolongo, P. & Maellaro, E. The autophagy inducer trehalose stimulates macropinocytosis in NF1-deficient glioblastoma cells. *Cancer Cell Int.* **22**, 232 (2022).
15. Yu, S., Park, H. & Kim, W. Trehalose Inhibits Inflammatory Responses through Mitochondrial Reprogramming in RAW 264.7 Macrophages. *Antioxidants*. **12**, (2023).
16. Hashemian, S. et al. The effects of oral trehalose on glycaemia, inflammation, and quality of life in patients with type 2 diabetes: a pilot randomized controlled trial. *Arch. Med. Sci.* **19**, 1693-1700 (2023).
17. Mizote, A. et al. Daily Intake of Trehalose Is Effective in the Prevention of Lifestyle-Related Diseases in Individuals with Risk Factors for Metabolic Syndrome. *J. Nutr. Sci. Vitaminol. (Tokyo).* **62**, 380-387 (2016).
18. Onyango, S. O. et al. Glycosidic linkage of rare and new-to-nature disaccharides reshapes gut microbiota in vitro. *Food Chem.* **411**, 135440 (2023).
19. Buckley, A. M. et al. Trehalose-Induced Remodelling of the Human Microbiota Affects Clostridioides difficile Infection Outcome in an In Vitro Colonic Model: A Pilot Study. *Front. Cell. Infect. Microbiol.* **11**, 670935 (2021).
20. Yang, N. et al. Hypertriglyceridaemia delays pancreatic regeneration after acute pancreatitis in mice and patients. *Gut*. **68**, 378-380 (2019).
21. Hosseinpour-Moghaddam, K., Caraglia, M. & Sahebkar, A. Autophagy induction by trehalose: Molecular mechanisms and therapeutic impacts. *J. Cell. Physiol.* **233**, 6524-6543 (2018).
22. Hu, F. et al. Macrophages in pancreatitis: Mechanisms and therapeutic potential. *Biomed. Pharmacother.* **131**, 110693 (2020).
23. Li, H., Wu, D., Zhang, H. & Li, P. New insights into regulatory cell death and acute pancreatitis. *Heliyon*. **9**, e18036 (2023).
24. Pupyshev, A. B., Klyushnik, T. P., Akopyan, A. A., Singh, S. K. & Tikhonova, M. A. Disaccharide trehalose in experimental therapies for neurodegenerative disorders: Molecular targets and translational potential. *Pharmacol. Res.* **183**, 106373 (2022).
25. Kul, E. & Stork, O. Trehalose consumption ameliorates pathogenesis in an inducible mouse model of the Fragile X-associated tremor/ataxia syndrome. *Nutr. Neurosci.*, 1-10 (2023).
26. Khamaysi, I. et al. S75 Combination of Trehalose and Heparanase Inhibitors Treatment Ameliorates Cerulein-Induced Acute Pancreatitis in a Murine Model. *The American Journal of*

Gastroenterology. **116**, S32 (2021).

27. Gesualdo, M. et al. Pancreatic Diseases and Microbiota: A Literature Review and Future Perspectives. *J. Clin. Med.* **9**, (2020).
28. Zhang, X. M. et al. Intestinal Microbial Community Differs between Acute Pancreatitis Patients and Healthy Volunteers. *Biomed. Environ. Sci.* **31**, 81-86 (2018).
29. Jin, M. et al. Colonic interleukin-22 protects intestinal mucosal barrier and microbiota abundance in severe acute pancreatitis. *Faseb. J.* **36**, e22174 (2022).
30. Zhao, T. et al. Impact of structurally diverse polysaccharides on colonic mucin O-glycosylation and gut microbiota. *Npj Biofilms Microbomes*. **9**, 97 (2023).
31. Lagkouvardos, I. et al. Sequence and cultivation study of Muribaculaceae reveals novel species, host preference, and functional potential of this yet undescribed family. *Microbiome*. **7**, 28 (2019).
32. Agus, A., Clement, K. & Sokol, H. Gut microbiota-derived metabolites as central regulators in metabolic disorders. *Gut*. **70**, 1174-1182 (2021).
33. Liu, J. et al. Integrative metagenomic and metabolomic analyses reveal the potential of gut microbiota to exacerbate acute pancreatitis. *Npj Biofilms Microbomes*. **10**, 29 (2024).
34. Arai, C. et al. Trehalose prevents adipocyte hypertrophy and mitigates insulin resistance. *Nutr. Res.* **30**, 840-848 (2010).
35. Yoshizane, C. et al. Daily consumption of one teaspoon of trehalose can help maintain glucose homeostasis: a double-blind, randomized controlled trial conducted in healthy volunteers. *Nutr. J.* **19**, 68 (2020).
36. Yaribeygi, H., Yaribeygi, A., Sathyapalan, T. & Sahebkar, A. Molecular mechanisms of trehalose in modulating glucose homeostasis in diabetes. *Diabetes Metab. Syndr.-Clin. Res. Rev.* **13**, 2214-2218 (2019).
37. Liu, S. et al. Trehalose attenuates renal ischemia-reperfusion injury by enhancing autophagy and inhibiting oxidative stress and inflammation. *Am. J. Physiol.-Renal Physiol.* **318**, F994-F1005 (2020).
38. Auger, J. P. et al. Metabolic rewiring promotes anti-inflammatory effects of glucocorticoids. *Nature*. **629**, 184-192 (2024).
39. Tan, S. et al. Trehalose alleviates apoptosis by protecting the autophagy-lysosomal system in alveolar macrophages during human silicosis. *Life Sci.* **257**, 118043 (2020).
40. Gong, Z. G., Wang, X. Y., Wang, J. H., Fan, R. F. & Wang, L. Trehalose prevents cadmium-induced hepatotoxicity by blocking Nrf2 pathway, restoring autophagy and inhibiting apoptosis. *J. Inorg. Biochem.* **192**, 62-71 (2019).
41. Tang, K. K., Liu, X. Y., Wang, Z. Y., Qu, K. C. & Fan, R. F. Trehalose alleviates cadmium-induced brain damage by ameliorating oxidative stress, autophagy inhibition, and apoptosis. *Metallomics*. **11**, 2043-2051 (2019).
42. Stahl, F., Evert, B. O., Han, X., Breuer, P. & Wullner, U. Spinocerebellar Ataxia Type 3 Pathophysiology-Implications for Translational Research and Clinical Studies. *Int. J. Mol. Sci.* **25**, (2024).

43. Collins, J. et al. Dietary trehalose enhances virulence of epidemic Clostridium difficile. *Nature*. **553**, 291-294 (2018).
44. Kawano, Y. et al. Microbiota imbalance induced by dietary sugar disrupts immune-mediated protection from metabolic syndrome. *Cell*. **185**, 3501-3519 (2022).
45. Fu, A. et al. Tumor-resident intracellular microbiota promotes metastatic colonization in breast cancer. *Cell*. **185**, 1356-1372 (2022).
46. Du, D. et al. Differences in glucose homeostasis and islet injury among diverse mice strains post acute pancreatitis. *Biochem. Biophys. Res. Commun.* **708**, 149780 (2024).
47. Barupal, D. K. & Fiehn, O. Chemical Similarity Enrichment Analysis (ChemRICH) as alternative to biochemical pathway mapping for metabolomic datasets. *Sci. Rep.* **7**, 14567 (2017).
48. Pang, Z. et al. MetaboAnalyst 6.0: towards a unified platform for metabolomics data processing, analysis and interpretation. *Nucleic. Acids. Res.*, (2024).
49. Lu, Y. et al. HDL inhibits pancreatic acinar cell NLRP3 inflammasome activation and protect against acinar cell pyroptosis in acute pancreatitis. *Int. Immunopharmacol.* **125**, 110950 (2023).

Figures

Figure 1

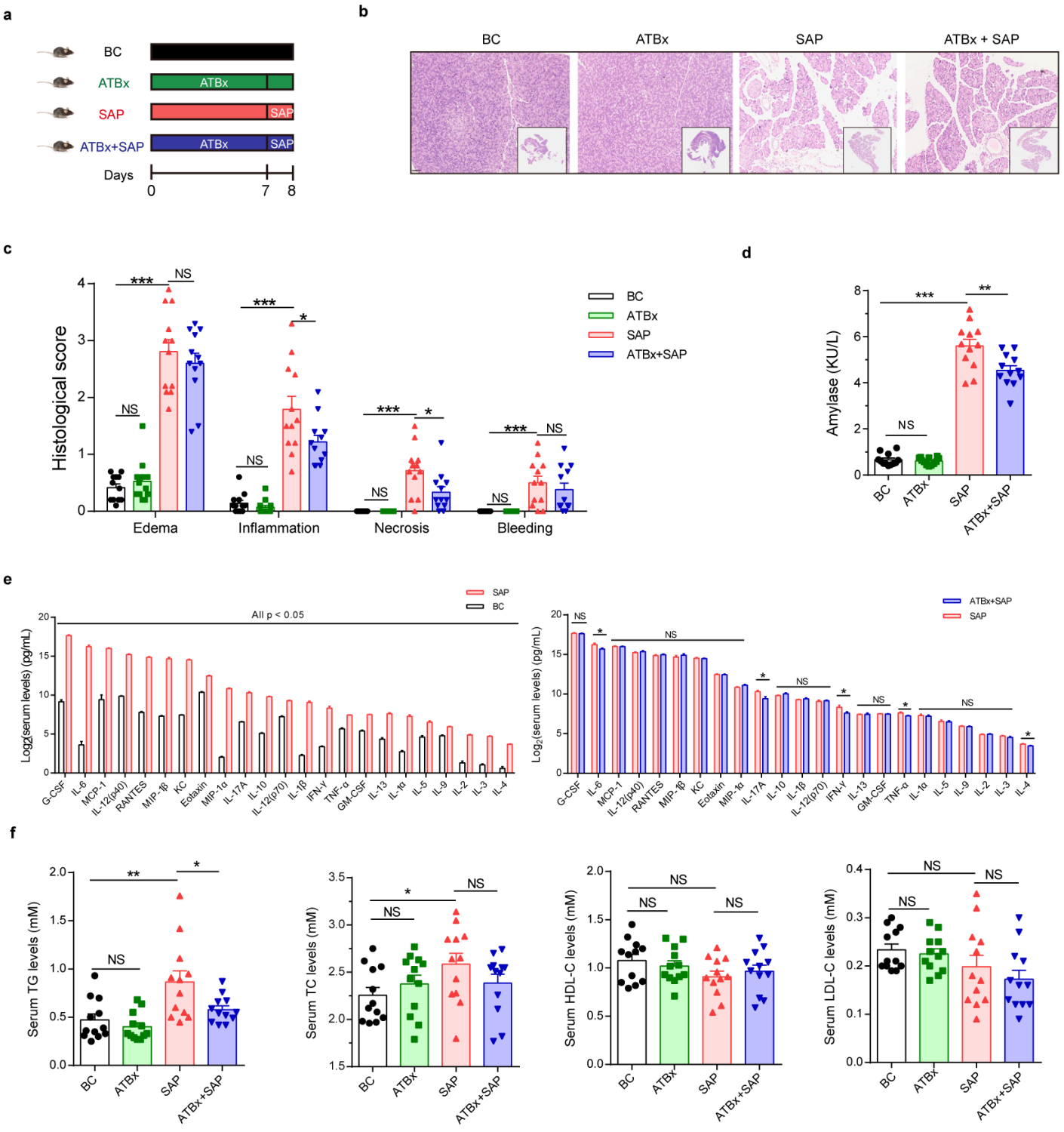

Figure 1

Bacterial depletion ameliorates pancreatic injury and the inflammatory response in SAP.

a Study design of ATBx treatment. **b** Representative images of H&E-stained pancreas sections. Scale bar = 50 μm. **c** Histological scores of H&E-stained pancreas sections (BC, n=12; ATBx, n=12; SAP, n=12; ATBx-SAP, n=12; two bio-repeats). **d** Serum amylase levels (12 mice/group). **e** Serum levels of 23

inflammatory cytokines profile in the groups (SAP vs. BC; ATBx-SAP vs. SAP). **f** Four key lipids levels: TG, TC, HDL-C, and LDL-C. $^{*}p < 0.05$, $^{**}p < 0.01$, $^{***}p < 0.001$. BC, blank control; SAP, severe acute pancreatitis; ATBx, antibiotic combination treatment; TG, triglyceride; TC, total cholesterol; HDL-C, high-density lipoprotein cholesterol; LDL-C, low-density lipoprotein cholesterol; HE, hematoxylin and eosin; NS, no significance.

Figure 2

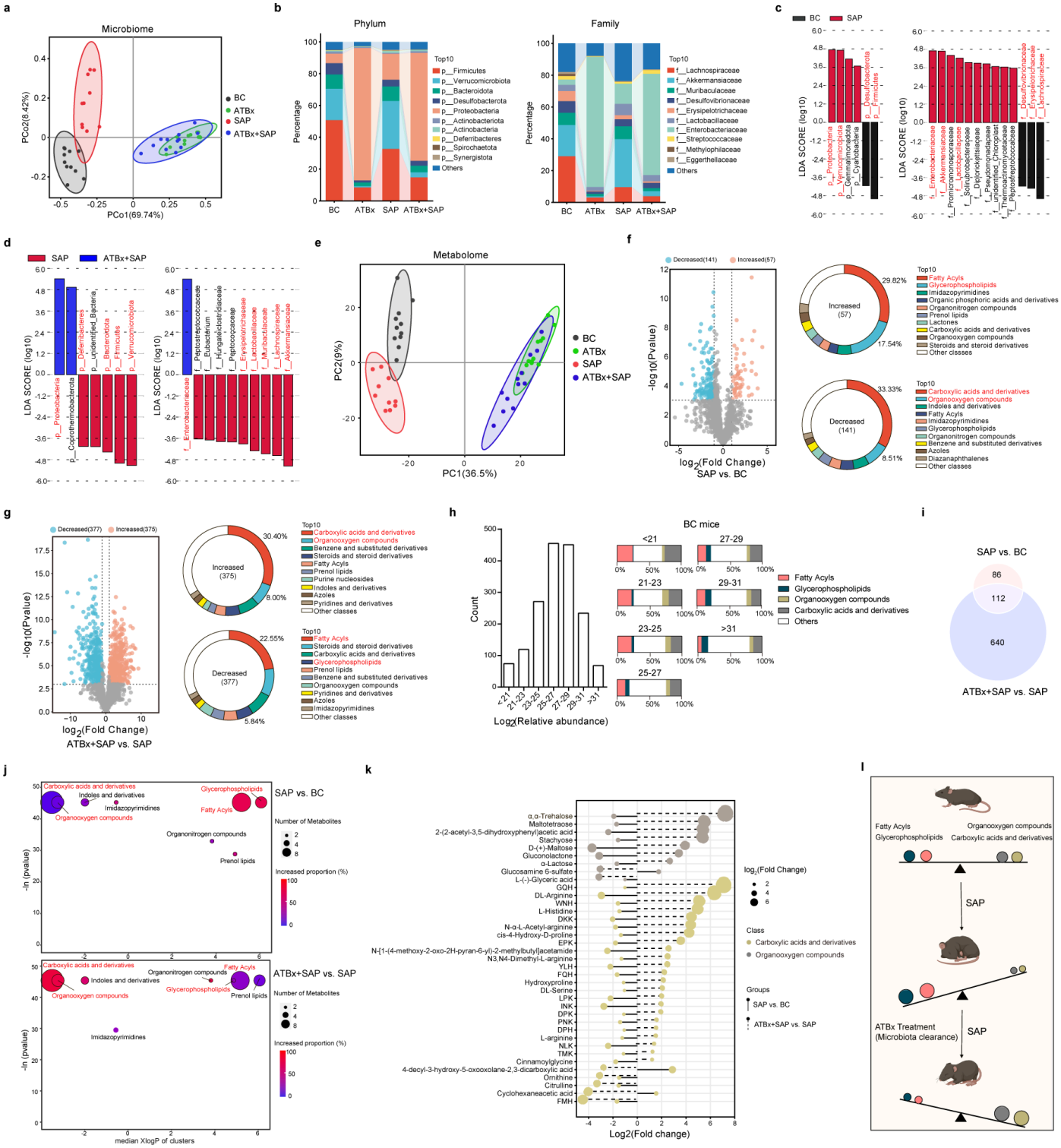

Bacterial depletion reverses SAP-induced gut microbial metabolism imbalance.

aPCoA plot of the gut microbiota from different groups (BC, n=11; ATBx, n=12; SAP, n=10; ATBx-SAP, n=12; two bio-repeats). **b** The top 10 microbial taxa in terms of abundance at the phylum and family levels (p: phylum, f: family). **c**, **d** Histogram of LDA distribution from LEfSe analysis for significantly different microorganisms in the SAP vs. BC and ATBx-SAP vs. SAP groups, and the microorganisms highlighted in red are among the top 10 in terms of abundance. **e** PCA plot of the gut microbial metabolism of the different groups (BC, n=11; ATBx, n=12; SAP, n=10; ATBx-SAP, n=12). **f, g** Volcano plot of microbial metabolites in the SAP vs. BC group and the ATBX-SAP vs. SAP group ($p < 0.001$, FC ≥ 2 or ≤ 0.5) and donut chart of differentially abundant metabolite class distributions. **h** Distribution histogram of overall microbial metabolism abundance in the BC group and the proportions of fatty acyls, glycerophospholipids, carboxylic acids, and derivatives & organooxygen compounds in the overall metabolite classes. **i** Venn diagram of all differentially abundant metabolites between the SAP vs. BC groups and between the ATBx -SAP vs.SAP groups. **j** Class enrichment of 112 metabolites with altered abundances identified by ChemRICH. The node size represents the total compound number for each cluster set, and the cluster color represents the proportion of compounds with increased abundance (red = increased, blue = decreased); only the enrichment clusters significantly differed at $p<0.05$ are shown. **k**Lollipop chart showing changes in the levels of carboxylic acids and derivatives &organooxygen compounds in the microbial metabolism of the SAP vs. BC group and the ATBx-SAP vs. SAP group. **l**Schematic diagram showing that ATBx treatment reversed SAP-induced microbial metabolismimbalance in the gut.PCoA: principal coordinate analysis, PCA: principal component analysis, ChemRICH: chemical similarity enrichment analysis, LEfSe: linear discriminant analysis effect size, LDA: linear discriminant analysis. XlogP: x-axis of mediation logarithmic additive octanol-water partition coefficients.

Figure 3

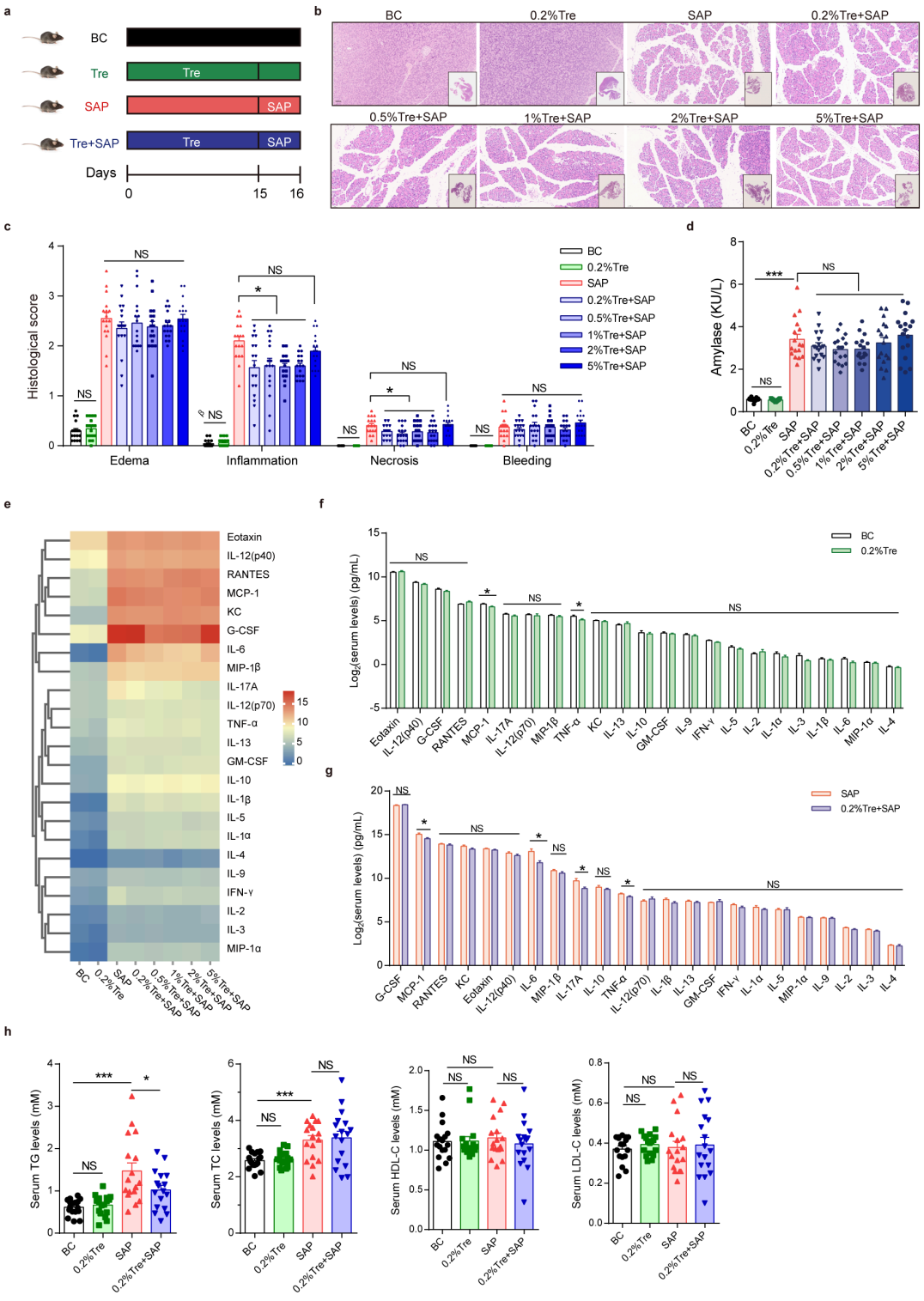

Figure 3

Trehalose ameliorates the severity of severe acute pancreatitis.

a Study design of the oral trehalose treatment. **b** Representative images of H&E-stained pancreas sections after oral trehalose treatment. Scale bar = 50 μm (BC, n=17; 0.2% Tre, n=17; SAP, n=17; 0.2% Tre-SAP, n=17; 0.5% Tre-SAP, n=17; 1% Tre-SAP, n=17; 2% Tre-SAP, n=17; 5% Tre-SAP, n=17; three bio-repeats).

c Histological scores of H&E-stained pancreas sections (17 mice/group). **d** Serum amylase levels after oral trehalose treatment in the SAP group. **e** Heatmap showing the changes in the levels of inflammatory factors in each group according to microarray data. **f**, **g** Serum levels of 23 inflammatory cytokines profile in the groups (0.2% Tre vs. BC; 0.2% Tre-SAP vs. SAP). **h** Levels of four key lipids after oral trehalose treatment (TG, TC, HDL-C, LDL-C). $^{*}p < 0.05$, $^{**}p < 0.01$, $^{***}p < 0.001$. Tre, trehalose; NS, no significance.

Figure 4

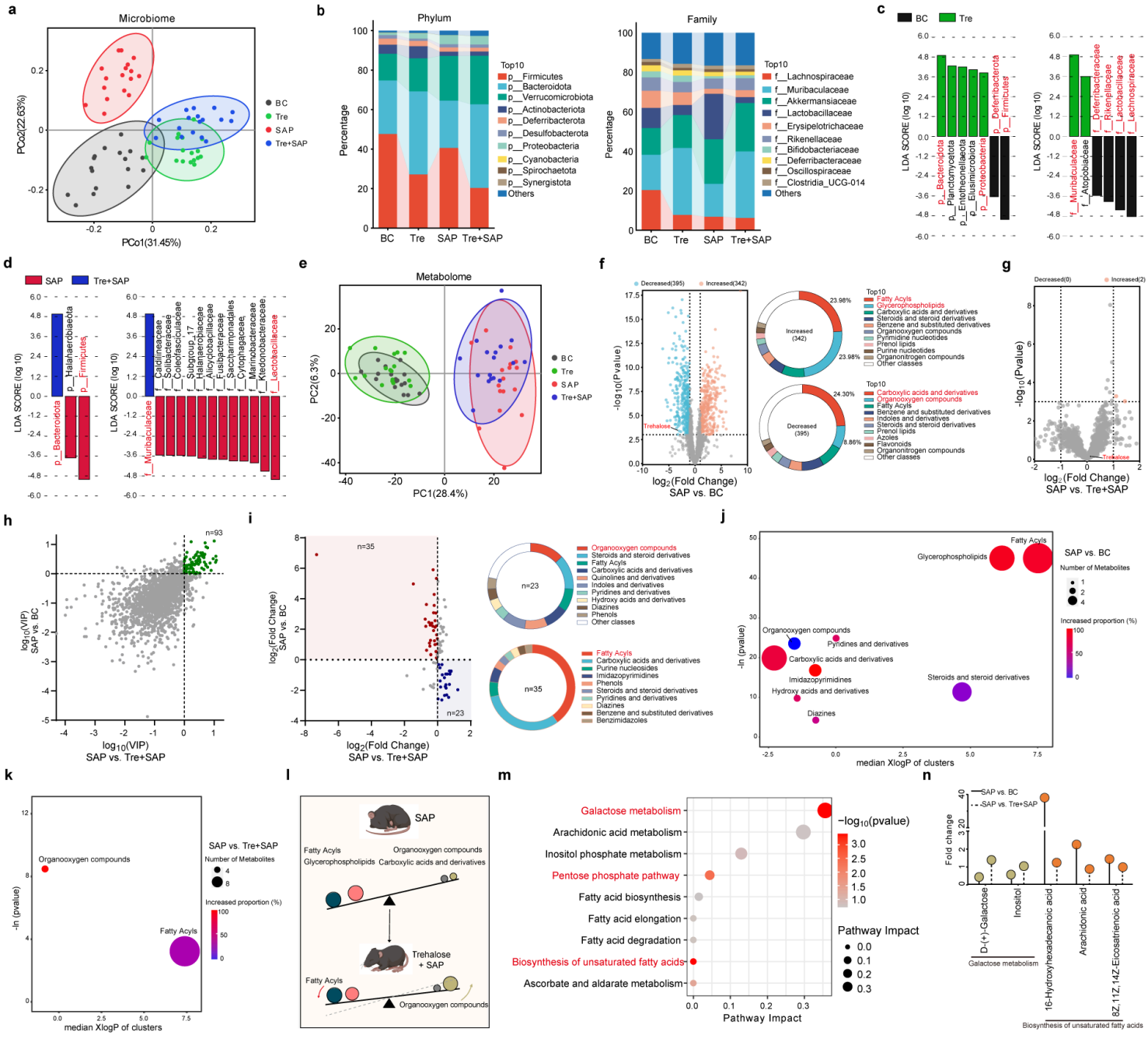

Figure 4

Trehalose modulates the gut microbial metabolism homeostasis in SAP.

aPCoA plot of the gut microbiota after oral trehalose treatment (BC, n=17; Tre, n=17; SAP, n=17; Tre-SAP, n=17; three bio-repeats). **b** The top 10 microbial taxa in terms of abundance at the phylum and family levels after oral trehalose treatment (p: phylum, f: family). **c**,**d** Histogram of LDA distribution from LEfSe analysis for significantly different microorganisms in the Tre vs. BC and Tre-SAP vs. SAP groups (LDA > 3.5); the microorganisms highlighted in red are among the top 10 most abundant microorganisms. **e** PCA plot of the gut microbial metabolism after oral trehalose treatment (BC, n=17; 0.2% Tre, n=17; SAP, n=17; 0.2% Tre-SAP, n=17). **f**,**g** Volcano plot of gut metabolites in the SAP vs. BC and Tre-SAP vs. SAP groups ($p < 0.001$, FC ≥ 2 or ≤ 0.5) and donut chart of differentially abundant metabolite class distributions. **h** VIP values for OPLS-DA of microbial metabolismin the Tre-SAP vs. SAP and SAP vs. BC groups, and VIP ≥ 1 was used as the threshold. **i** The square grid shows the changes in 93 differentially abundant metabolites in the intersection of the Tre-SAP vs. SAP group and SAP vs. BC group(blue: FC>1 in the Tre-SAP vs. SAP group & FC<1 in the SAP vs. BC group; red: FC<1 in the Tre-SAP vs. SAP group &FC>1 in the SAP vs. BC group). **j**, **k** ChemRICH class enrichment of 93 differentially abundant metabolites in the intersection of Tre-SAP vs. SAP and SAP vs. BC groups. **l** Schematic diagram showing that oral trehalose treatment ameliorated SAP-induced microbial metabolismimbalance. **m** Pathway analysis of differentially abundant metabolites was performed with MetaboAnalyst 6.0. **n** The levels of key metabolites of significantly different pathways (galactose metabolism and biosynthesis of unsaturated fatty acids) in the Tre-SAP vs. SAP and SAP vs. BC groups. OPLS-DA orthogonal partial least squares-discriminant analysis, VIP variable influence on projection, FC fold change.

Figure 5

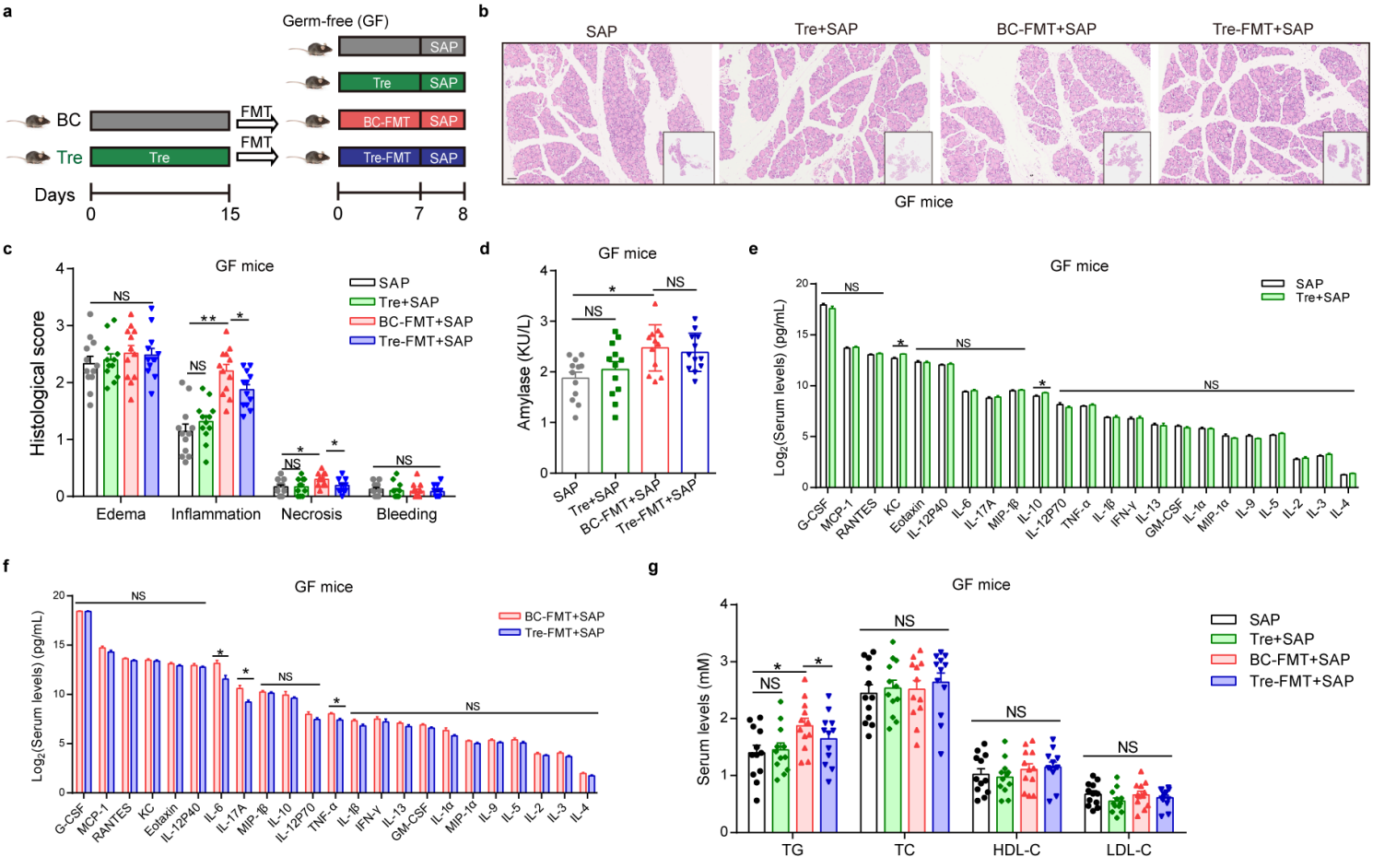

Figure 5

Trehalose ameliorates SAP in a gut microbiota-dependent manner.

a Study design of the FMT experiment in GF mice. **b** Representative images of H&E-stained pancreas sections after FMT in GF mice with SAP. Scale bar = 50 μm (SAP, n=12; Tre-SAP, n=12; BC-FMT-SAP, n=12; Tre-FMT-SAP, n=12; two bio-repeats). **c** Histological scores of H&E-stained pancreas sections after FMT in GF mice with SAP (12 mice/group). **d** Serum amylase levels in each group of GF mice. **e**, **f** Serum levels of 23 inflammatory cytokines profile in GF mice with SAP (Tre--SAP vs. SAP; Tre-FMT--SAP vs. BC-FMT--SAP). **g** Four lipids levels after FMT in GF mice with SAP (TG, TC, HDL-C, LDL-C). $^{*}p < 0.05$, $^{**}p < 0.01$, $^{***}p < 0.001$. FMT, fecal microbiota transplantation; NS, no significance.

Figure 6

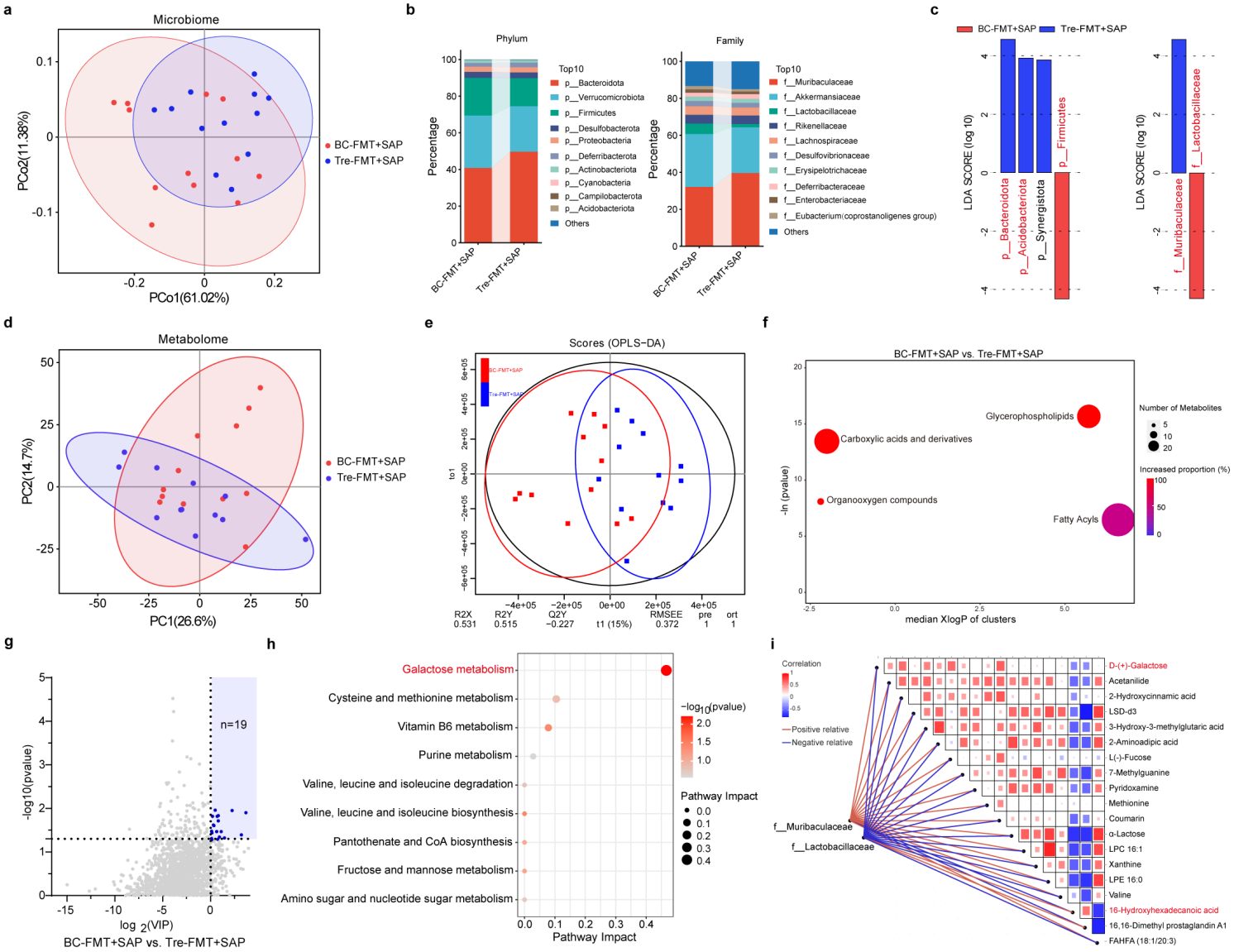

Figure 6

Galactose metabolism and Muribaculaceae are key factors in trehalose-induced "microbial metabolism-gut-pancreatic axis".

aPcoA plot of the gut microbiota after FMT in GF mice with SAP (Tre-FMT-SAP, n=12; BC-FMT-SAP, n=12; two bio-repeats). **b** The top 10 microbial taxa in terms of abundance at the phylum and family levels after Tre-FMT in GF mice with SAP (p: phylum, f: family). **c** LEFSe shows differentially abundant bacterial taxa between the Tre-FMT--SAP and BC-FMT-SAP groups, and the LDA score of the differentially abundant bacterial taxa (LDA > 3.5). **d** PCA plot of the gut microbial metabolismafter FMT in GF mice with SAP (Tre-FMT-SAP, n=12; BC-FMT-SAP, n=12). **e** Score plot for OPLS-DA after FMT in GF mice with SAP; each point represents an individual mouse. **f** ChemRICH class enrichment of VIP>1 differentially abundant metabolites in the Tre-FMT-SAP vs. the BC-FMT-SAP group. **g** Nineteen significantly differentially abundant metabolites in the Tre-FMT-SAP group vs. BC-FMT-SAP group (VIP >1 and p<0.05). **h** Pathway analysis of differentially abundant metabolites was performed with MetaboAnalyst 6.0. **i** A network heatmap of correlations between 19 significantly differentially abundant metabolites and differential bacterial taxa.

Figure 7

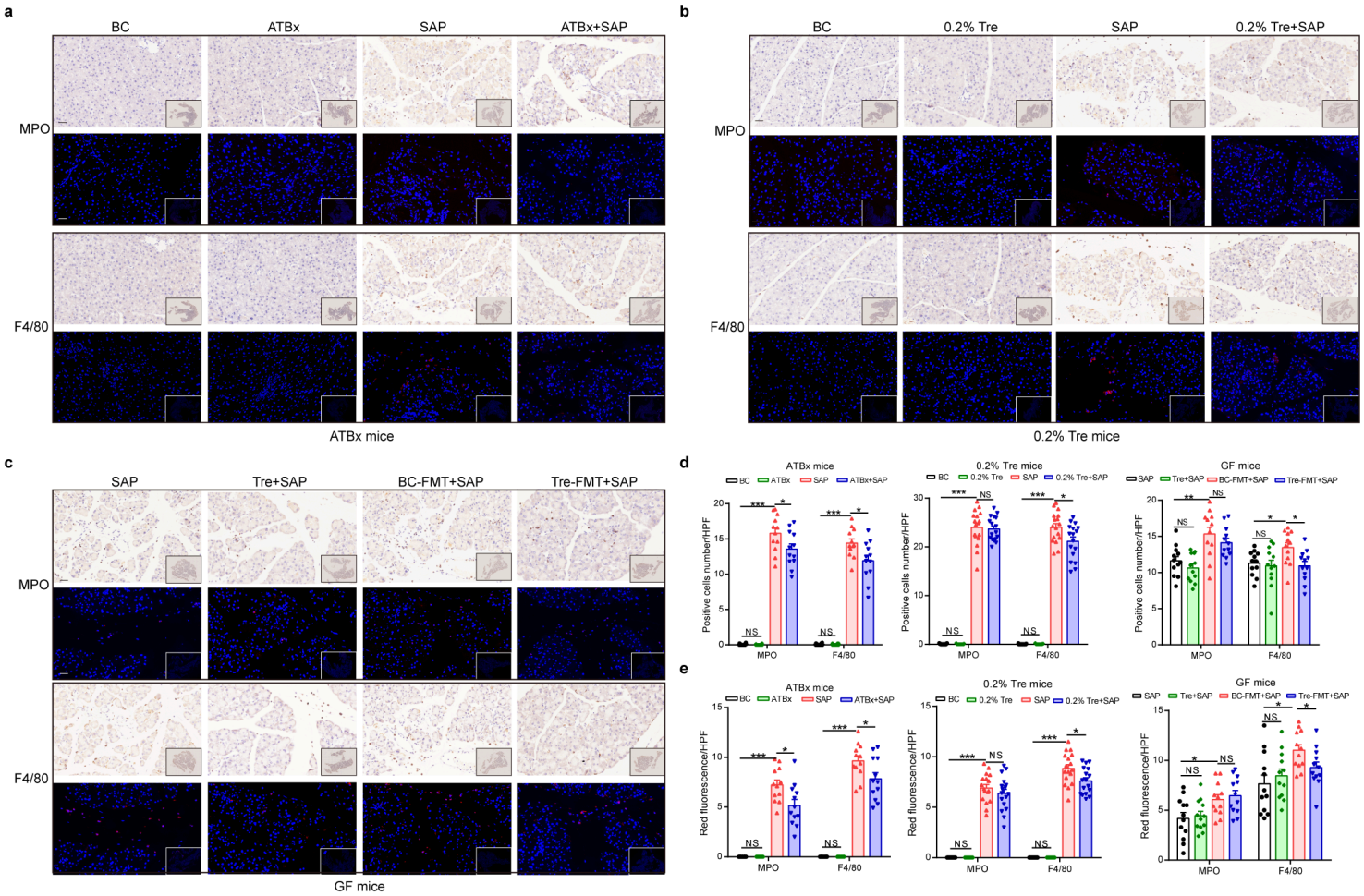

Figure 7

Trehalose reduces macrophage infiltration in the pancreas.

a-c Representative IHC and IF images of MPO and F4/80 staining in the pancreas after ATBx treatment, oral trehalose treatment, and FMT (scale bar = 20 μm). **d**, **e** IHC and IF quantification of MPO and F4/80

staining in the pancreas after ATBx treatment, oral trehalose treatment, and FMT (each point represents an individual mouse). $^{*}p < 0.05$, $^{**}p < 0.01$, $^{***}p < 0.001$. NS, no significance.

Figure 8

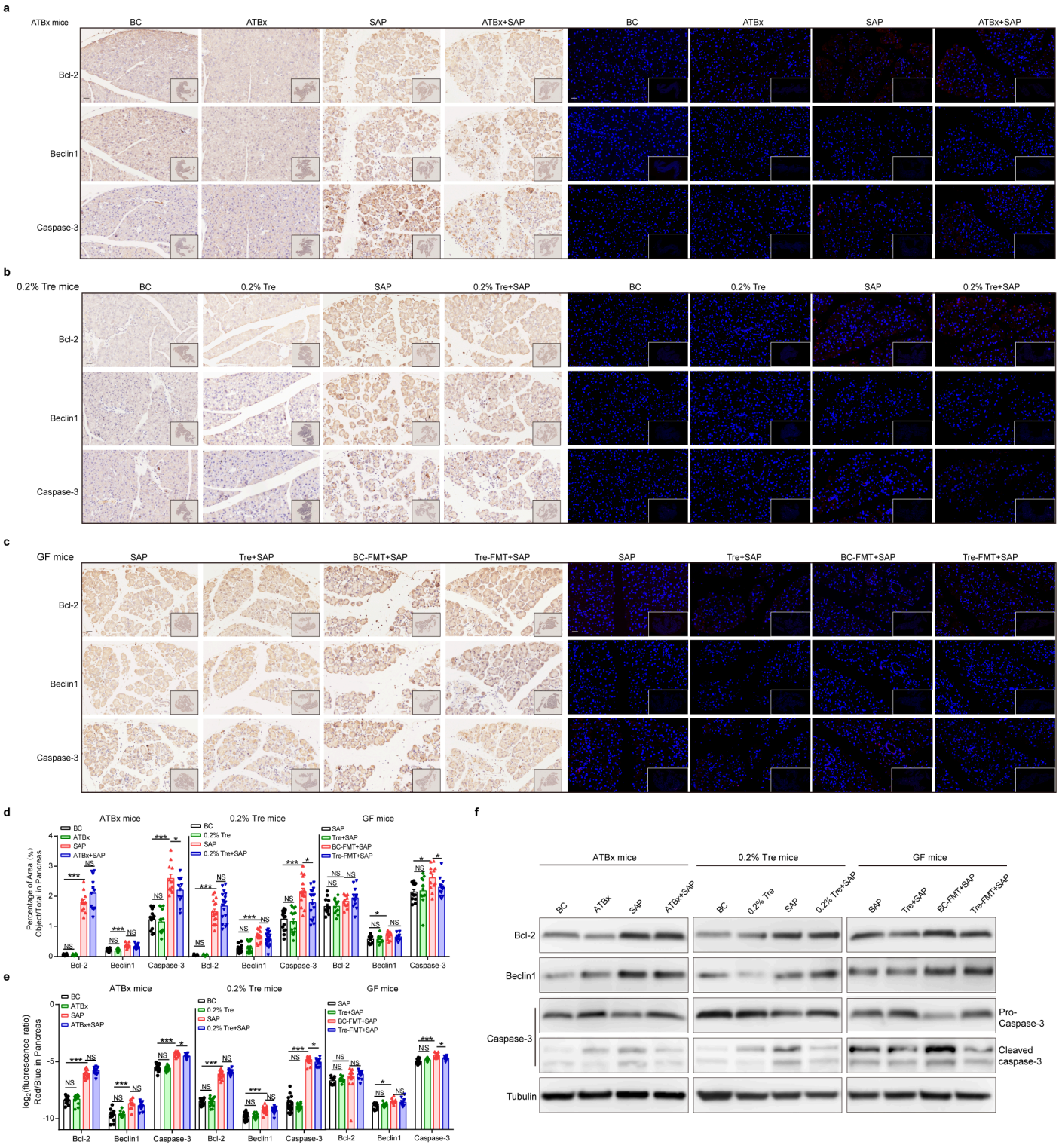

Figure 8

Trehalose reduces caspase-3-mediated apoptosis in the pancreas.

a-c Representative IHC and IF images of Bcl-2, Beclin-1, and caspase-3 expression staining in the pancreas after ATBx treatment, oral trehalose treatment, and FMT (scale bar = 20 μm). **d**, **e** IHC and IF quantification of Bcl-2, Beclin-1, and caspase-3 expression staining in the pancreas after ATBx treatment, oral trehalose treatment, and FMT. **f** Western blot images of Bcl-2, Beclin-1, caspase-3, and Tubulin protein expression in the pancreas after ATBx treatment, oral trehalose treatment, and FMT. $^{*}p < 0.05$, $^{**}p < 0.01$, $^{***}p < 0.001$. NS, no significance.

Figure 9

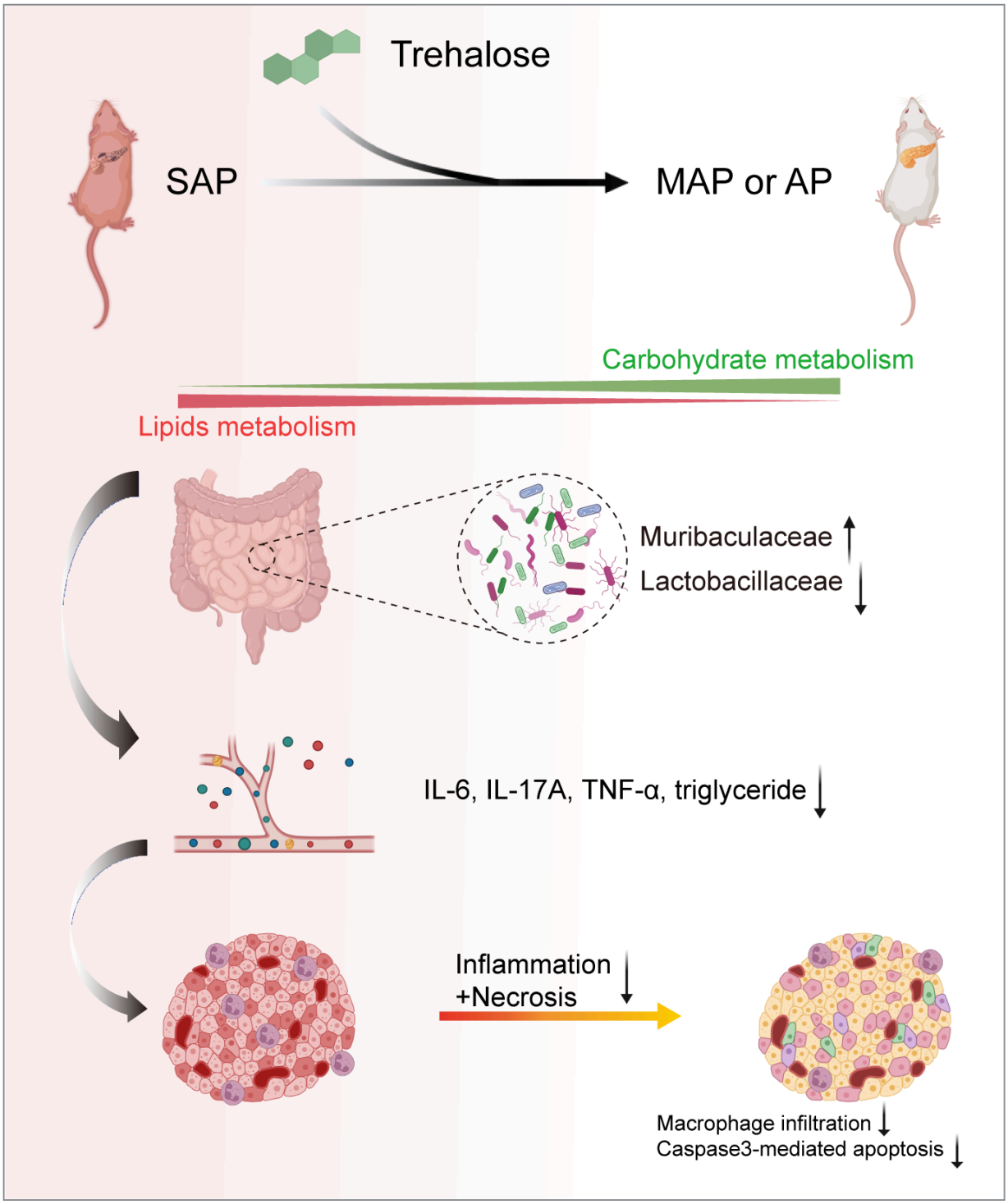

Figure 9

Legend not included with this version

Supplementary Files

This is a list of supplementary files associated with this preprint. Click to download.

- SupplementaryFigure1.tif
- SupplementaryFigure2.tif
- SupplementaryFigure3.tif
- SupplementaryFigure4.tif
- SupplementaryFigure5.tif
- SupplementaryFigure6.tif
- SupplementaryFigurelegends.docx
- SupplementaryTable1.xlsx
- SupplementaryTable2.xlsx
- SupplementaryTable3.xlsx
- SourceData.xlsx